

Mean Life of the Metastable 2^3P_1 State of the Two-Electron Fluorine Ion*

J. Richard Mowat, I. A. Sellin, R. S. Peterson, and D. J. Pegg

The University of Tennessee, Knoxville, Tennessee 37916

Oak Ridge National Laboratory, Oak Ridge, Tennessee 37830

Matt D. Brown and James R. Macdonald

Kansas State University, Manhattan, Kansas 66506

(Received 2 February 1973)

By measuring the radiative decay in flight of a foil-excited heliumlike fluorine beam, we have determined the lifetime of the metastable 2^3P_1 state of the two-electron ion F^{7+} . Our data yield the singlet-triplet intercombination transition probability

$$A(1^1S_0-2^3P_1) = (1.77 \pm 0.10) \times 10^9 \text{ sec}^{-1},$$

which is in excellent agreement with theoretical calculations of a strongly Z -dependent spin-orbit-induced electric dipole decay, and extends our earlier measurements for ions in this isoelectronic sequence. Because this transition is observed in the solar spectrum for all abundant heliumlike ions from carbon to iron, we also discuss the relevance of this measurement to solar physics.

I. INTRODUCTION

The $1^1S_0-2^3P_1$ intercombination transition in the two-electron atomic system is accompanied by a change in the atomic spin angular momentum. In the nonrelativistic limit such a decay cannot proceed by electric dipole ($E1$) radiation because of the $\Delta S=0$ selection rule. The parity change that occurs when the atomic state changes from P to S , together with the $\Delta S=0$ selection rule, makes magnetic dipole ($M1$) decay doubly forbidden. Nevertheless, this intercombination line has been known ever since it was first observed by Lyman¹ in neutral helium almost 50 years ago. Although the wavelength of this 592-Å (He I) line has been measured to high precision,² its small branching ratio has, until recently,³ precluded a measurement of the $1^1S_0-2^3P_1$ decay probability.

The observation of heliumlike intercombination lines in the emission spectra of highly stripped ions in both laboratory plasmas and solar corona stimulated attempts to compute the associated decay rates.^{4,5} It was found that singlet-triplet mixing by the (relativistic) spin-orbit interaction allows the 2^3P_1 state to decay to the ground state by $E1$ emission. Subsequent measurements⁶ of the $1^1S_0-2^3P_1$ transition probability in two-electron nitrogen and oxygen ions were consistent with the theoretical estimates. In this paper an extension of this work along the isoelectronic sequence to $Z=9$ is reported. The Z dependence of the transition probability is so strong that a change of Z of only one unit ($Z=8$ to $Z=9$) is accompanied by more than a threefold increase

in the decay rate. The results of the present experiment are in good agreement with theoretical predictions.^{4,5}

II. THEORY

When the (relativistic) spin-orbit interaction is included in the Hamiltonian of the two-electron atom, the total orbital and spin angular momenta cease to be constants of the motion. The resulting breakdown of the LS coupling approximation causes a mixing of the singlet and triplet states of the same parity and total angular momentum $\vec{J} = \vec{L} + \vec{S}$. Thus the 2^3P_1 state is no longer a pure triplet state but contains admixtures of all singlet P_1 states⁵:

$$|2^3P_1\rangle = |2^3P_1\rangle_0 - \sum_{n=2}^{\infty} \frac{\langle 2^3P_1 | H_3 | n^1P_1 \rangle_0}{E(n^1P_1) - E(2^3P_1)} |n^1P_1\rangle_0,$$

where the subscript 0 denotes the pure state in the absence of spin-orbit effects, and H_3 is the spin-orbit part of the Breit Hamiltonian in Pauli approximation.⁷ Following Drake and Dalgarno,⁵ we neglect the smaller spin-spin interaction. This impure state can decay to the ground state by $E1$ emission. Clearly the $E1$ decay rate will depend upon how much of the perturbed wave function has singlet character.

The results of a variational calculation⁵ appear to scale approximately as Z^{10} in the region $3 \leq Z \leq 10$. The rough argument given below helps elucidate the origin of this Z^{10} dependence. Assuming that the nearby 2^1P_1 state is the dominant admixture,⁸ the perturbed 2^3P_1 wave function can

be approximated by

$$|2^3P_1\rangle \approx |2^3P_1\rangle_0 - \epsilon |2^1P_1\rangle_0,$$

where the mixing parameter ϵ is defined as

$$\epsilon \equiv \frac{\langle 2^3P_1 | H_3 | 2^1P_1 \rangle_0}{E(2^1P_1) - E(2^3P_1)}.$$

The E1 transition rate is

$$A(1^1S_0 - 2^3P_1) \propto |\langle 2^3P_1 | \vec{r}_1 + \vec{r}_2 | 1^1S_0 \rangle|^2$$

or

$$A(1^1S_0 - 2^3P_1) \propto |\epsilon|^2 |\langle 2^1P_1 | \vec{r}_1 + \vec{r}_2 | 1^1S_0 \rangle_0|^2.$$

Hence,

$$A(1^1S_0 - 2^3P_1) \approx |\epsilon|^2 A(1^1S_0 - 2^1P_1),$$

where we have made the additional approximation

$$\nu(2^3P_1 - 1^1S_0) = \nu(2^1P_1 - 1^1S_0).$$

For sufficiently large Z , for which a hydrogenic approximation is appropriate, the singlet decay rate $A(1^1S_0 - 2^1P_1)$ will scale approximately as Z^4 . The remainder of the $\sim Z^{10}$ dependence in the triplet decay rate appears in ϵ . The singlet-triplet energy separation in the denominator of ϵ is just the exchange integral K which scales⁹ as Z^1 for large Z . The leading term in H_3 arises from the nuclear contribution to the spin-orbit interaction which is proportional to $\sum_i (Z/r_i^3) \vec{r}_i \cdot \vec{S}_i$, where the i th electron has position \vec{r}_i , orbital angular momentum \vec{L}_i , and spin \vec{S}_i . Since matrix elements of r_i^{-3} scale as Z^3 , the matrix element of H_3 will scale as Z^4 , barring accidental cancellation of the leading terms. Such a cancellation is not expected to occur, since this nuclear contribution has even symmetry with respect to the operations of parity and electron exchange. We conclude that $|\epsilon|^2 \propto (Z^4/Z)^2 = Z^6$, and $A(1^1S_0 - 2^3P_1) \propto Z^{10}$.

Because of this strong Z dependence, the decay rate increases by more than a factor of 3 just going from $Z=8$ to $Z=9$. At $Z=7$ the intercombination transition becomes the dominant channel for depopulating the 2^3P_1 state. At $Z=9$ it is 20 times more probable than the competing fine-structure transition¹⁰ $2^3S_1 - 2^3P_1$ (which is a fully allowed E1 decay). For $Z=6$ and beyond these two are the only important decay channels, since the 2^1S_0 level then lies above the 2^3P_1 state (the very weak $2^3P_1 - 2^3P_0$ M1 transition can be neglected).

III. EXPERIMENT

The lifetime of the 2^3P_1 state was determined by measuring the exponential decay in flight of the 732-eV $1^1S_0 - 2^3P_1$ line emitted by a beam of fast, foil-excited, two-electron fluorine ions. The

intensity of this line was proportional to the 2^3P_1 state population at time t , which was related to the distance x along the beam from the point of excitation through $x=vt$ ($t=0$ at the foil). In the absence of cascading effects and backgrounds from other $n=2$ to $n=1$ transitions, the intensity decay could be fitted to $e^{-\lambda x}$. From the inverse decay length $\lambda^{-1} \equiv v\tau$ and the beam velocity v , the mean life τ is easily determined.

The 2^3P_1 state was produced by passing a beam of fluorine ions through a thin carbon foil. Such beams emerge from the foil in a variety of excited states, mostly corresponding to charge states +5 through +9, the actual distribution depending upon the incident beam energy.¹¹ Allowed radiative transitions from such ions have mean lives typically in the 10^{-11} - to 10^{-13} -sec range, so that by simply beginning observations ≤ 1 cm downstream from the target, backgrounds from allowed transitions and short-lived cascade effects were effectively eliminated. Most of the backgrounds which remained (e.g., fluorescence of vacuum chamber walls due to penetrating high-energy cosmic rays, nuclear γ rays from Coulomb excitation and photons from other metastable beam particles) were not detected, since the energy discrimination of the Si(Li) detector was sufficient to separate out all x rays except those with energies corresponding to K -series transitions in fluorine ions, and since the detector output pulses were processed by a biased amplifier to screen out both low-energy noise pulses and high-energy photon signals.

IV. APPARATUS

Fluorine beams of energy 15 MeV (incident charge state +3), 25 MeV (+4), and 43 MeV (+6) obtained from the ORNL tandem Van de Graaff accelerator were directed through a thin ($\sim 10 \mu\text{g}/\text{cm}^2$) carbon foil which could be moved parallel to the beam direction (see Fig. 1). Collimation of emitted x rays reduced the field of view of the Si(Li) detector to a section of beam about $\frac{1}{2}$ cm long. Photon counts were normalized to the integrated beam current that was collected in a biased Faraday cup.

An important feature of this apparatus is the use of a Si(Li) detector (ORTEC model 7116) in the low-energy region where the F^{7+} x ray is located (732 eV). Even though the 0.0005 in Be window attenuated the x-ray signal by an estimated 99%, the solid-state detector was found to have a much larger detection efficiency than the Bragg-crystal, gas-flow proportional counter arrangement used in previous experiments.⁶ The superior efficiency is due to improved solid angle and signal transmission associated with the elimination of long

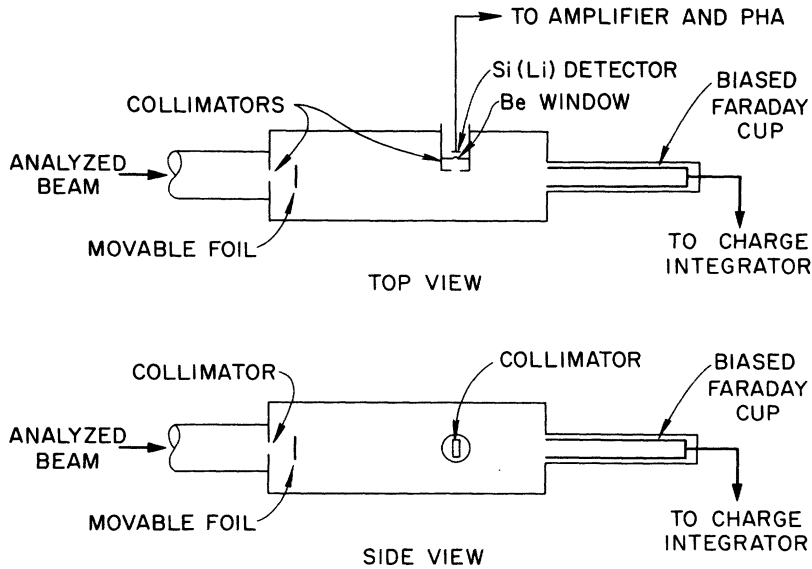


FIG. 1. Schematic diagram of the apparatus.

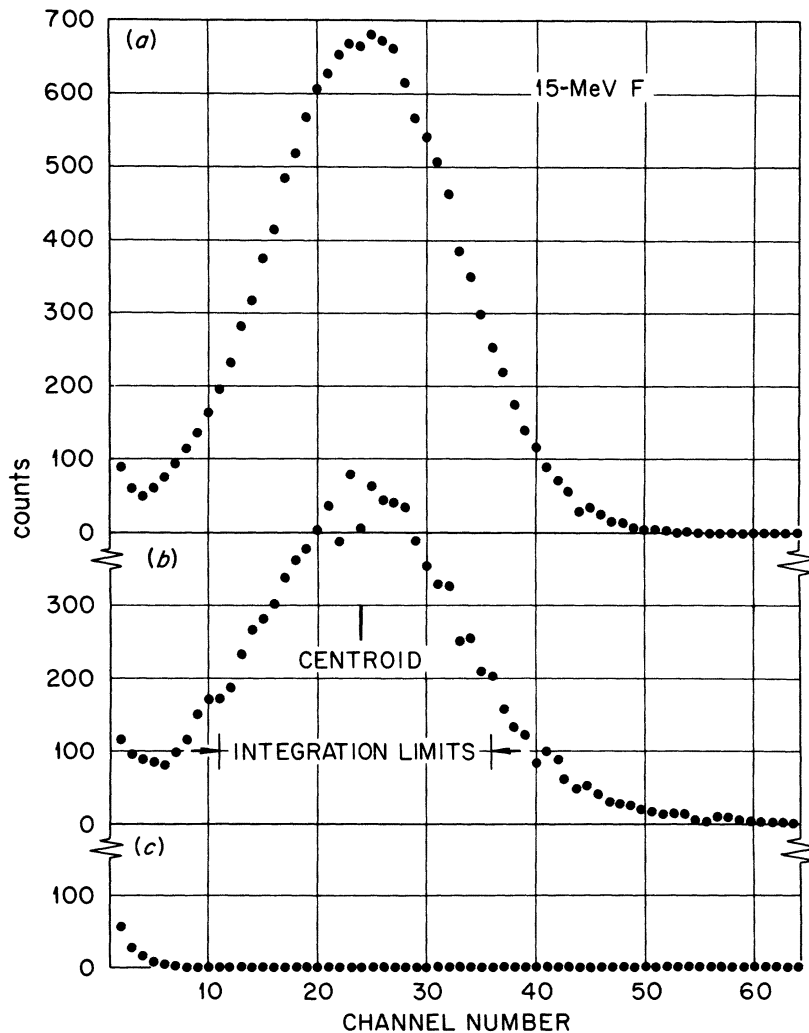


FIG. 2. Pulse-height spectra normalized to 240 sec counting time. (a) Pulser simulated 722-eV x ray; (b) typical emission spectrum from beam; (c) noise counts accumulated with x-ray simulator and beam off. Channel 48 corresponds to 1 keV, and the dispersion is 11.7 eV/channel.

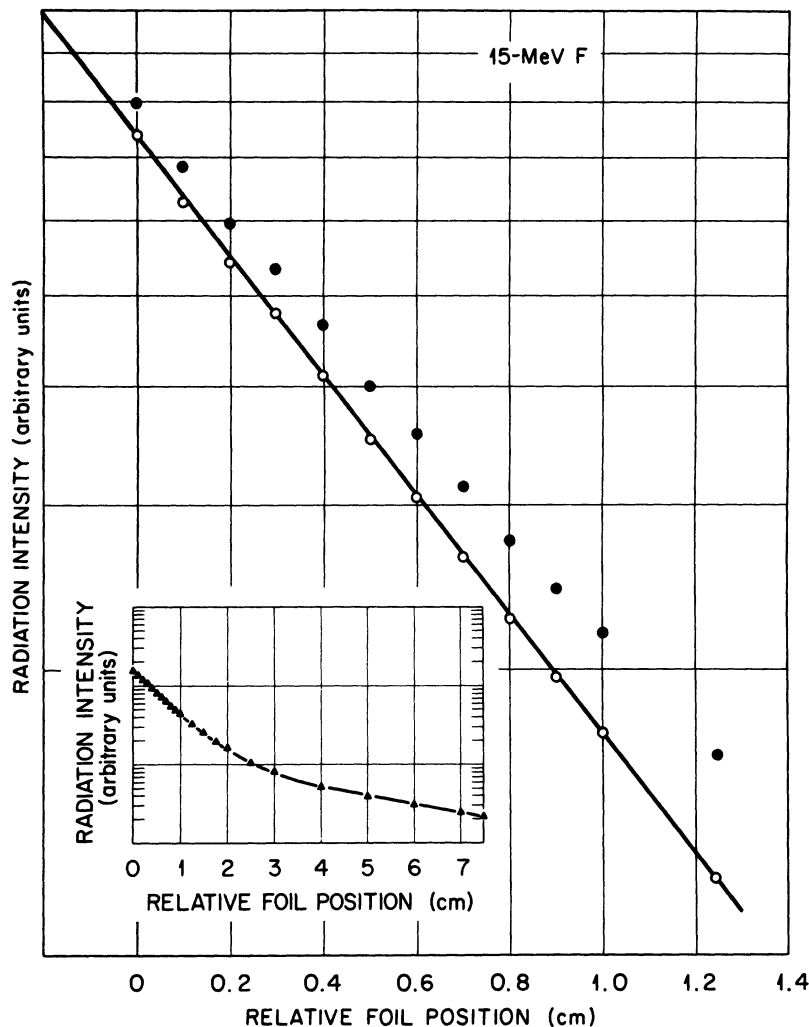


FIG. 3. Experimental decay curve at 15 MeV beam energy. The inset shows the full curve fitted to a sum of two decaying exponentials (solid line). Closed circles are uncorrected data and open circles are data after subtraction of the apparent background, which has been represented to a useful degree of accuracy by a single exponential. The statistical counting errors are smaller than the circles. The solid line passing through the open circles is a least-squares fit to a single, decaying exponential.

collimators and poorly reflecting crystals. Unlike the proportional counter, the Si(Li) detector is insensitive to background counts from high-energy cosmic rays.

Although the *energy* resolution of the present detector is poorer than one employing a crystal spectrometer, the apparatus provides *spatial* resolution in the sense that the relative populations of neighboring states vary considerably with position downstream because of their different lifetimes. The three decays $1^1S_0-2^3S_1$, $1^1S_0-2^3P_2$, and $1^1S_0-2^3P_1$ could not be resolved energetically using a crystal spectrometer without severe intensity loss, but they can be spatially resolved because the ratio of decay lengths of the states is approximately 500 000:22:1. Hence, near the foil, the 2^3P_2 and 2^3S_1 intercombination decays are too slow to seriously mimic the 2^3P_1 decay. Since our earlier experiments on two-electron oxygen established the correctness of this line

identification procedure, we felt it unnecessary to perform a tedious, statistically limiting photon energy analysis.

A monoenergetic x ray that is absorbed in the sensitive volume of the lithium-drifted silicon diode produces an electrical pulse whose height is proportional to the x-ray energy. Noise in this sensitive volume, together with other electronic factors mentioned below, causes a (Gaussian) distribution of pulse heights about the true value. Figure 2(b) presents such a pulse-height spectrum, taken at 15 MeV beam energy. For comparison, an electronically simulated 722-eV x-ray spectrum is shown in Fig. 2(a). To obtain this spectrum a calibrated, linear pulser (ORTEC model 731) was used at the detector preamplifier test input (i.e., in place of detector output pulses), all other electronic elements remaining unchanged. The *energy-independent* width of the pulser spectrum is a function of preamplifier noise and amplifier

time constants; it represents the contribution of the detection electronics to the system resolution. The total system resolution also contains an energy-dependent contribution from ionization statistics in the Si(Li) diode. Pulser spectra taken at two different energies serve to establish the energy scale. The centroids of the two peaks [Figs. 2(a) and 2(b)] are virtually indistinguishable within the ~ 240 -eV (full width at half-maximum) resolution. The spectrum shown as Fig. 2(c), taken with beam and x-ray pulse simulator off, demonstrates the existence of a small, exponentially decreasing noise tail near the low-energy end of the spectrum. All three of these curves are normalized to the same counting time. The intensity was chosen to be proportional to the number of counts occurring between the integration limits shown [Fig. 2(b)]. These are located symmetrically with respect to the centroid of a typical, high-statistics spectrum. This choice

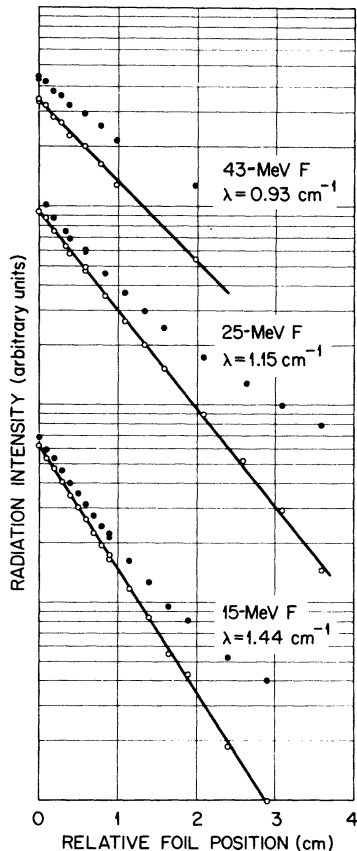


FIG. 4. Experimental decay curves. The closed circles are uncorrected data and the open circles are data after subtraction of a single, decaying-exponential background. The statistical counting errors are smaller than the circles. The solid line is a least-squares fit to a single, decaying exponential.

of integration limits minimizes intensity changes due to possible small foil-position-dependent centroid shifts. For purposes of analyzing the line intensity as a function of foil position, the intensity was normalized to an arbitrary integrated beam current.

V. RESULTS

The decay curve obtained at 15 MeV beam energy is shown in the inset of Fig. 3. Data were taken in a random sequence of foil positions in order to average out possible foil-aging effects.⁶ The solid line in the inset is a least-squares fit to a sum of two decaying exponentials.

The fast-decaying component is identified as the $1^1S_0-2^3P_1$ decay on the basis of (a) the photon energy, which implies that the decay is an $n=2 \rightarrow n=1$ transition, (b) the intensity of the decay as a function of beam energy, which strongly suggests that the emitting ion has charge state +7 (at 43 MeV charge states $\leq +6$ account for $\leq 1\%$ of the beam), (c) the consistency of the measured decay length with that predicted by scaling the previously measured O^{5+} and N^{6+} transition rates,⁶ and (d) the scaling of the decay length with beam energy, which verifies that the effects of cascades and backgrounds from other decays have been rendered negligible in comparison with the quoted experimental error.

The slowly decaying component is, so far, unidentified, and it may in fact contain more than one exponential component. It appears to decay too rapidly to be attributed to the $1^1S_0-2^3P_2$ $M2$ decay¹² which should be present as a background. One possible source for this decay is the feeding of the $2P$ level by a cascade that originates in a state of sufficiently large n and $l=n-1$ such that the first step $n \rightarrow n-1$ proceeds in a time that is long compared to the 2^3P_1 lifetime. Fortunately

TABLE I. Experimental results. The average lifetime $\tau = 0.536(30)$ nsec implies a total decay rate $(1.87 \pm 0.10) \times 10^9 \text{ sec}^{-1}$.

Beam energy ^a (MeV)	Beam velocity v (10^9 cm/sec)	Inverse decay length λ (cm^{-1})	Lifetime $\tau = 1/v\lambda$ (nsec)
15.4	1.25	1.44(4)	0.555(15)
25.5	1.61	1.15(4)	0.540(19)
42.8	2.09	0.93(5)	0.514(28)

^aEnergy loss in the foil has been neglected. The uncertainty in the listed lifetime is significantly larger than that due to this small and imperfectly known correction.

the fitted decay length of the fast component is very insensitive to the precise decay length assigned to the slow (presumed single) exponential background.

The closed circles are experimental points, and the open circles are data that have been corrected by subtracting off a single, slowly decaying exponential. In all cases, the point diameter exceeds the statistical error bars. The line drawn through the open circles is a least-squares fit to a single decaying exponential. Similar results were obtained at 25 and 43 MeV beam energy (Fig. 4).

The three values for the 2^3P_1 lifetime obtained in this way are recorded in Table I. The uncertainties quoted represent the uncertainty in the fitted decay length. The accuracy decreases at high velocities because of the presence of persistent, short-lived cascades. The proper scaling with beam energy is evident, and we take as our final result a simple average of these three lifetimes,

$$\tau(2^3P_1) = 0.536(20) \text{ nsec.}$$

VI. DISCUSSION

Subtraction of the known $2^3S_1-2^3P_1$ transition probability¹⁰ $0.0915 \times 10^9 \text{ sec}^{-1}$ from our experimental value for $\tau^{-1} = (1.87 \pm 0.10) \times 10^9 \text{ sec}^{-1}$ gives

an experimental result for the spin-orbit-induced $E1$ transition probability

$$A(1^1S_0-2^3P_1) = (1.77 \pm 0.10) \times 10^9 \text{ sec}^{-1},$$

which agrees with the variational result $1.85 \times 10^9 \text{ sec}^{-1}$ of Drake and Dalgarno⁵ and the semiempirical result $(1.7 \pm 0.2) \times 10^9 \text{ sec}^{-1}$ of Elton.⁴ About 8% of the variational result is due to mixing of 2^3P_1 with singlet states of $n > 2$.

The intercombination transition discussed here is observed in the solar spectrum of all abundant elements between carbon and iron.¹³ The intensity of this transition relative to that of $1^1S_0-2^3S_1 M1$ transition is used in the determination of the electron density in solar active regions.¹⁴ According to Jordan¹³ the precise value of $A(1^1S_0-2^3P_1)$ is important for this density determination only up to about $Z = 10$. As discussed above, the $2^3S_1-2^3P_1$ transition is the dominant radiative decay for $Z \leq 6$. The present measurement at $Z = 9$ therefore falls within the most critical region $7 \leq Z \leq 10$.

Note added in proof. The $F^{7+} 2^3P_1$ lifetime has been remeasured by Richard *et al.*¹⁵ Even though they employ a crystal spectrometer to energetically resolve both singlet and triplet He-like as well as Li-like $2p-1s$ decays, they too, find that the 2^3P_1 decay curve is not a single exponential. This result supports our claim that the slow component of the decay curve is a cascade effect.

*Research supported in part by the Office of Naval Research, the National Aeronautics and Space Administration, and by Union Carbide Corporation and Oak Ridge Associated Universities under contract with the U.S. Atomic Energy Commission.

¹T. Lyman, *Astrophys. J.* **60**, 1 (1924).

²G. Herzberg, *Proc. R. Soc. A* **248**, 309 (1958).

³H. Y. S. Tang and W. Happer, *Bull. Am. Phys. Soc.* **17**, 476 (1972).

⁴R. C. Elton, *Astrophys. J.* **148**, 573 (1967).

⁵G. W. F. Drake and A. Dalgarno, *Astrophys. J.* **157**, 459 (1969).

⁶I. A. Sellin, Bailey L. Donnally, and C. Y. Fan, *Phys. Rev. Lett.* **21**, 717 (1968); and I. A. Sellin, Matt Brown, Winthrop W. Smith, and Bailey Donnally, *Phys. Rev. A* **2**, 1189 (1970).

⁷Hans A. Bethe and Edwin E. Salpeter, *Quantum Mechanics of One- and Two-Electron Atoms* (Springer-Verlag, New York, 1957), p. 181.

⁸The computations in Ref. 4 are based upon this assumption, and the resulting decay probabilities are only 8% smaller than the more accurate ones computed in Ref. 5 using the full expansion.

⁹Reference 7, p. 135.

¹⁰W. L. Wiese, M. W. Smith, and B. M. Glennon, *Atomic Transition Probabilities*, NSRDS-NBS 4 (U. S. GPO, Washington, D. C., 1966), Vol. 1, p. 125.

¹¹J. B. Marion and F. C. Young, *Nuclear Reaction Analysis* (North-Holland, Amsterdam, 1968), p. 44.

¹²G. F. W. Drake, *Astrophys. J.* **158**, 1199 (1969); V. L. Jacobs, *J. Phys. B* **5**, 213 (1972); R. Marrus and R. W. Schmieder, *Phys. Rev. A* **5**, 1160 (1972).

¹³C. Jordan, private communication; and unpublished.

¹⁴A. H. Gabriel and C. Jordan, *Mon. Not. R. Astron. Soc.* **145**, 241 (1969).

¹⁵Patrick Richard, R. L. Kauffman, F. F. Hopkins, C. W. Woods, and K. A. Jamison, *Phys. Rev. Lett.* **30**, 888 (1973).